Katholieke Universiteit Leuven

Departement Elektrotechniek ESAT-SISTA/TR 08-216

Comparative evaluation of howling detection criteria in notch-filter-based howling suppression[1]

Toon van Waterschoot[2] [3] and Marc Moonen[2]

May 2009
Published in *Preprints of the AES 126th Convention*, Munich, Germany, May 2009, Preprint no. 7752, 16 p.

[1]This report will be available by anonymous ftp by Dec. 2009 from *ftp.esat.kuleuven.be* in the directory *pub/sista/vanwaterschoot/reports/08-216.pdf*

[2]K.U.Leuven, Dept. of Electrical Engineering (ESAT), Research group SCD(SISTA), Kasteelpark Arenberg 10, 3001 Leuven, Belgium, Tel. +32 16 321927, Fax +32 16 321970, WWW: *http://homes.esat.kuleuven.be/∼tvanwate*. E-mail: *toon.vanwaterschoot@esat.kuleuven.be.*

[3]This research work was carried out at the ESAT laboratory of the Katholieke Universiteit Leuven, in the frame of K.U.Leuven Research Council CoE EF/05/006 Optimization in Engineering (OPTEC) and the Belgian Programme on Interuniversity Attraction Poles, initiated by the Belgian Federal Science Policy Office IUAP P6/04 (DYSCO, 'Dynamical systems, control and optimization', 2007-2011), and was supported by the Institute for the Promotion of Innovation through Science and Technology in Flanders (IWT-Vlaanderen). The scientific responsibility is assumed by its authors.

Audio Engineering Society

Convention Paper 7752

Presented at the 126th Convention
2009 May 7–10 Munich, Germany

The papers at this Convention have been selected on the basis of a submitted abstract and extended precis that have been peer reviewed by at least two qualified anonymous reviewers. This convention paper has been reproduced from the author's advance manuscript, without editing, corrections, or consideration by the Review Board. The AES takes no responsibility for the contents. Additional papers may be obtained by sending request and remittance to Audio Engineering Society, 60 East 42nd Street, New York, New York 10165-2520, USA; also see www.aes.org. All rights reserved. Reproduction of this paper, or any portion thereof, is not permitted without direct permission from the Journal of the Audio Engineering Society.

Comparative evaluation of howling detection criteria in notch-filter-based howling suppression

Toon van Waterschoot[1] and Marc Moonen[1]

[1] *Dept. E.E./ESAT, SCD-SISTA, Katholieke Universiteit Leuven, Kasteelpark Arenberg 10, B-3001 Leuven, Belgium*

Correspondence should be addressed to Toon van Waterschoot
(toon.vanwaterschoot@esat.kuleuven.be)

ABSTRACT

Notch-filter-based howling suppression (NHS) is one of the most popular methods for acoustic feedback control in public address and hands-free communication systems. The NHS method consists of two stages: howling detection and notch filter design. While the design of notch filters is based on well-established filter design techniques, there is little agreement in the NHS literature on how the howling detection subproblem should be tackled. Moreover, since the NHS literature mainly consists of patents, only few experimental results have been reported. The aim of this paper is to describe a unifying framework for howling detection, and to provide a comparative evaluation of existing and novel howling detection criteria.

1. INTRODUCTION

The acoustic feedback problem is a long-standing problem in sound reinforcement applications such as public address and hands-free communication systems. When a sound signal is captured by a microphone, and subsequently amplified and played back through a loudspeaker, the loudspeaker sound is often fed back to the microphone either through a direct acoustic coupling or indirectly as a consequence of reverberation. The existence of such an acoustic feedback path results in a closed signal loop, which limits the performance of a sound reinforcement system in two ways. First of all, there is an upper limit to the amount of amplification that can be applied if the system is required to remain stable, which is referred to as the maximum stable gain (MSG). Second, the sound quality is affected by occasional howling when the MSG is exceeded, or, even when the

system is operating below the MSG, by ringing and excessive reverberation.

State-of-the-art methods for acoustic feedback control can be categorized into four classes [1]: phase modulation methods, gain reduction methods, spatial filtering methods, and room modeling methods. Gain reduction methods are without any doubt the most widespread solution for acoustic feedback control in sound reinforcement systems. These methods attempt to automate the actions that a human operator would undertake for preventing or eliminating howling in a sound reinforcement system. These actions usually consist in reducing the electro-acoustic forward path gain, such that the system moves away from the point of instability. Depending on the width of the frequency band in which the gain is actually reduced, we can discriminate between three gain reduction methods [1]: in *automatic gain control (AGC)* methods [2]-[4], the gain is reduced equally in the entire frequency range, while in *automatic equalization (AEQ)* methods [4]-[10], a gain reduction is applied only in critical subbands (i.e., subbands in which the loop gain of the sound reinforcement system is close to unity), and in *notch-filter-based howling suppression (NHS)* methods [11]-[23], the gain is reduced in narrow frequency bands around critical frequencies (i.e., frequencies at which the loop gain is close to unity).

Every gain reduction method has to be activated in some way, when a closed-loop instability or a tendency towards instability is detected. Most gain reduction methods are reactive, in the sense that howling can usually be perceived before it is actually detected. In these methods, howling detection is typically based on a combined spectral and temporal analysis of the microphone signal. Due to the sinusoidal nature of howling, the microphone signal frequency components having the largest magnitude are considered to be candidate howling components. The true howling components within this set of candidates can then be discriminated from the source signal tonal components (originating from voiced speech or musical tones) using several criteria. Spectral criteria for discriminating between howling and tonal components are based on one or more of the following features: the power ratio of the candidate howling component and the entire spectrum [5]-[7],[14]-[16],[18]-[23], the power ratio of the candidate howling component and its (sub-)harmonics [12]-[15],[17], and the power ratio of the candidate howling component and its neighboring frequency components [4],[8]-[10]. On the other hand, temporal criteria for howling detection rely on the observation that howling components typically persist for a longer time than tonal components [2],[3],[11]-[13],[16]-[20] and exhibit an exponentially increasing magnitude until the sound reinforcement system saturates [8]-[10].

The goal of this paper is twofold. First of all, we want to evaluate the existing howling detection criteria in an objective way. This can be achieved by reformulating the howling detection problem as a binary hypothesis test and hence evaluating the detection performance using standard measures from detection theory (e.g., the receiver operating characteristic (ROC) curve [24, Ch. 3]). Such an evaluation has not been reported earlier, and is necessary to make a fair comparison between existing howling detection methods and to highlight their shortcomings. A second goal consists in the development of novel howling detection criteria that are particularly suited for audio applications. In [1], it was found that most of the existing howling detection criteria suffer from an intolerably high probability of false alarm when the microphone signal is an audio signal. This is due to the fact that it is much harder to discriminate howling components from tonal audio components than from voiced speech components. False alarms result in the unnecessary activation of notch filters, which can be detrimental for the sound quality [1].

This paper is organized as follows. In Section 2, we outline the NHS method for acoustic feedback control, which consists of two stages: howling detection and notch filter design. Six microphone signal features that have been proposed for howling detection are then defined in a formal way in Section 3. These features are used in Section 4 to rederive the existing howling detection criteria, and to develop novel howling detection criteria. Both the existing and novel howling detection criteria are then objectively evaluated and compared, and appropriate values for the detection thresholds are suggested. In Section 5, a selection of the existing and novel howling detection criteria are applied in an NHS computer simulation to assess the acoustic feedback control perfor-

mance in terms of the achievable MSG increase, the sound quality, and the reliability. Finally, Section 6 concludes the paper. We should note that, while the focus of this paper is on NHS methods, the proposed howling detection criteria can also be applied to other gain reduction methods such as AGC and AEQ methods.

2. NOTCH-FILTER-BASED HOWLING SUPPRESSION

The NHS method for acoustic feedback control can be outlined as shown in Fig. 1 for a sound reinforcement system with one loudspeaker and one microphone. Here, $F(q,t)$ and $G(q,t)$ denote the transfer functions of the acoustic feedback path and the electro-acoustic forward path, respectively, with q the time shift operator, i.e., $q^{-k}u(t) = u(t-k)$. The source signal $v(t)$ is picked up by the microphone, together with the feedback signal $x(t) = F(q,t)u(t)$. The resulting microphone signal $y(t) = v(t)+x(t)$ is subsequently amplified and processed in the electro-acoustic forward path to yield the loudspeaker signal $u(t) = G(q,t)y(t)$. In the NHS method, the microphone signal $y(t)$ is first processed by a howling detection algorithm, which forwards a set of design parameters $\mathcal{D}_H(t)$ to a bank of adjustable notch filters $H(q,t)$ that is inserted in the electro-acoustic forward path such that $u(t) = H(q,t)G(q,t)y(t)$. The concept of howling detection and notch filter design is described below, closely following [1].

2.1. Howling detection

We assume that the howling detection is performed in a frame-based manner, on microphone signal frames with a frame length of M samples and a frame hop size of P samples (i.e., a frame overlap of $M-P$ samples). At time t, the data in the microphone signal frame can then be represented by the vector

$$\mathbf{y}(t) = \begin{bmatrix} y(t+P-M) & \dots & y(t+P-1) \end{bmatrix}^T \quad (1)$$

and the short-term microphone signal spectrum can be obtained as the DFT of the data in $\mathbf{y}(t)$, i.e.,

$$Y(\omega_k, t) = \sum_{n=0}^{M-1} w(t_n)y(t_n)e^{-j\omega_k t_n}, \quad k = 0, \dots, M-1 \quad (2)$$

with $\omega_k \triangleq 2\pi k/M$ and $t_n \triangleq t+P-M+n$. The microphone signal DFT in (2) is generally calculated using the FFT algorithm, and includes a window function $w(t_n)$ to reduce the spectral leakage [25] (e.g., a Blackman window has succesfully been applied to audio signal processing [26][1]). The choice of the signal framing parameters M and P has a rather profound influence on the performance of the howling detection. Small values for the frame length M have been proposed to allow for very quick howling detection (e.g., $M = 128$, corresponding to 4 ms at $f_s = 32$ kHz [8]-[10]), such that howling may potentially be detected before it is actually perceived [8]-[10]. On the other hand, larger values for M provide a better frequency resolution in the microphone signal DFT spectrum estimate (e.g., $M = 4096$, corresponding to 92.9 ms at $f_s = 44.1$ kHz [12],[13] or to 85.3 ms at $f_s = 48$ kHz [19]), which is necessary when working with very narrowband notch filters such as the 1/60 octave filters used in [21],[22]. A large frame hop size P may result in a large time lag between howling detection and notch filtering, unless a P-sample delay is inserted in the electro-acoustic forward path. On the other hand, a small value for P leads to an increase in computational complexity since the howling detection algorithm is

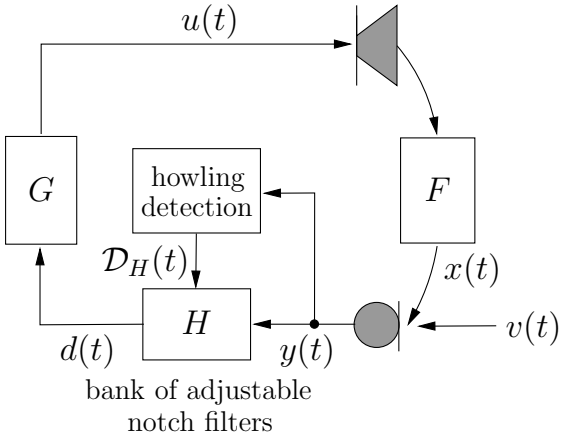


Fig. 1: Notch-filter-based howling suppression (NHS) by feeding the microphone signal to a howling detection algorithm, which forwards a set of design parameters $\mathcal{D}_H(t)$ to a bank of adjustable notch filters $H(q,t)$ that is inserted in the electro-acoustic forward path.

[1] http://ccrma.stanford.edu/~jos/mdft/Use_Blackman_Window.html

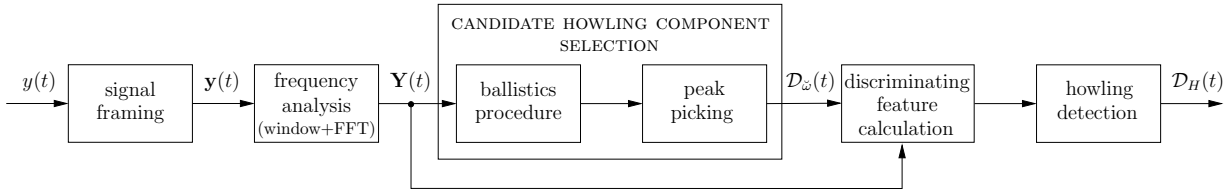


Fig. 2: NHS howling detection: from the microphone signal $y(t)$, a set of notch filter design parameters $\mathcal{D}_H(t)$ is calculated.

then executed more often. Generally, a 25–50 % frame overlap ($P = 3M/4, \ldots, M/2$) is found to be a good compromise.

A pre-defined number N of spectral peaks is identified from the DFT magnitude spectrum estimate, with N typically chosen in the range 1–10. These N frequency components are termed "candidate howling components" and their radial frequency values are collected in the set $\mathcal{D}_{\breve{\omega}}(t) = \{\breve{\omega}_i\}_{i=1}^{N}$. A spectral peak picking algorithm is usually applied to find the candidate howling components. A more advanced approach consists in selecting frequency components that have a consistently increasing magnitude in successive signal frames. This is possible by applying a so-called "ballistics" procedure [19] before executing the peak picking algorithm. A number of spectral and temporal features are then calculated and combined in a howling detection criterion to determine whether a candidate howling component indeed corresponds to a howling component or rather to a source signal tonal component, see Section 3-4 for more details. The complete howling detection procedure is summarized in Fig. 2.

2.2. Notch filter design

When howling has been detected, a notch filter has to be activated to suppress the howling component and stabilize the closed-loop system. The most commonly used notch filter structure in NHS is the second-order IIR (i.e., biquadratic) filter structure,

$$H_l(q,t) = \frac{b_l^{(0)}(t) + b_l^{(1)}(t)q^{-1} + b_l^{(2)}(t)q^{-2}}{1 + a_l^{(1)}(t)q^{-1} + a_l^{(2)}(t)q^{-2}}. \quad (3)$$

The bank of adjustable notch filters that is inserted in the electro-acoustic forward path, as shown in Fig. 1, then consists of a cascade of $n_H/2$ such filters, i.e.,

$$H(q,t) = \prod_{l=1}^{n_H/2} H_l(q,t) \quad (4)$$

with n_H the resulting order of the cascade filter.

The notch filter design procedure consists of two parts: first the set of design parameters $\mathcal{D}_H(t)$ delivered by the howling detection algorithm has to be mapped to a set of filter specifications, which are then translated into filter coefficient values. A biquadratic notch filter has five coefficients, which depend on a set of six filter specifications [27]: the (radial) center frequency $\omega_{c,l}$, the (radial) bandwidth B_l, the notch gain $G_{c,l}$, the gain at the band edges $G_{B,l}$, the gain at DC $G_{0,l}$, and the gain at the Nyquist frequency $G_{\pi,l}$. If we fix the latter two variables to $G_{0,l} = G_{\pi,l} = 0$ dB and the gain at the band edges to $G_{B,l} = G_{c,l} + 3$ dB in case $G_{c,l} \leq -6$ dB, or to $G_{B,l} = G_{c,l}/2$ in case $G_{c,l} \geq -6$ dB (thereby adopting Moorers bandwidth definition [28]), then only the first three filter specifications remain.

The set of design parameters $\mathcal{D}_H(t)$ should always contain the radial frequencies $\{\breve{\omega}_i\}_{i\in\mathcal{I}_H(t)}$ of the howling components that have been identified in the howling detection algorithm, where $\mathcal{I}_H(t) \subseteq \{1, \ldots, N\}$ denotes the set of indices for which howling has been detected. For each howling component, a notch filter should be activated, with a center frequency corresponding to the howling frequency. The DFT magnitude values $\{|Y(\breve{\omega}_i)|\}_{i\in\mathcal{I}_H(t)}$ may also be contained in the set of design parameters $\mathcal{D}_H(t)$ since these values can be used to determine the notch gain $G_{c,l}$. However, it is common practice to work with fixed notch gain values that are independent of the howling component magnitude. Typically, when a new howling component has been

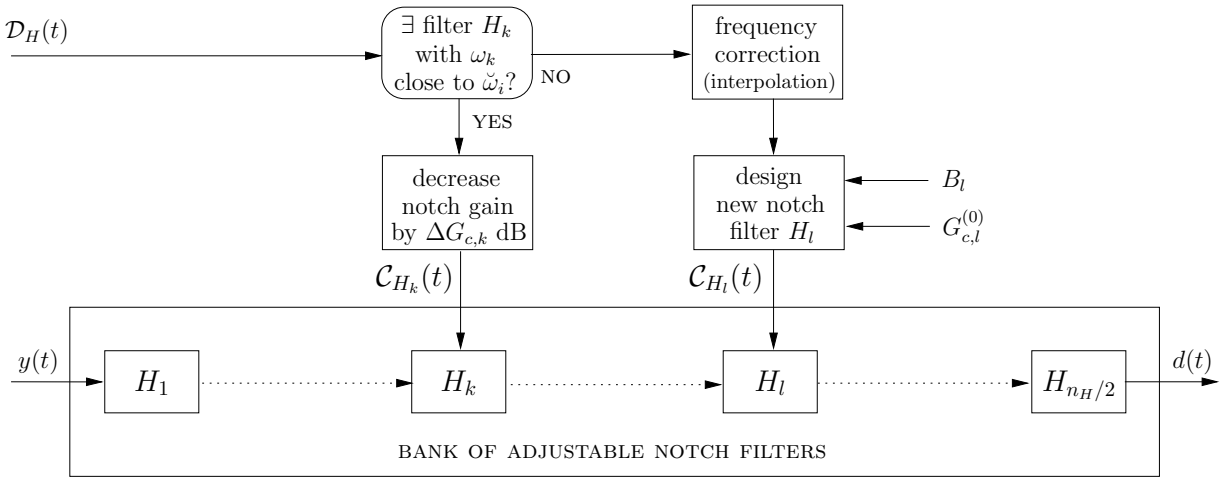


Fig. 3: NHS notch filter design: the microphone signal $y(t)$ is filtered in a bank of adjustable notch filters, designed using the design parameters in $\mathcal{D}_H(t)$, resulting in the howling-compensated signal $d(t)$.

detected (i.e., a howling component at a frequency that has not occured before), the notch gain is set to an initial value $G_{c,l}^{(0)}$, e.g., $G_{c,l}^{(0)} = -3$ dB [12],[13] or $G_{c,l}^{(0)} = -6$ dB [19]. If howling persists or reoccurs at a frequency close to a previously identified howling frequency, then the gain is decreased with $\Delta G_{c,l}$ dB, e.g., $\Delta G_{c,l} = -3$ dB [12],[13] or $\Delta G_{c,l} = -6$ dB [19]. The radial notch filter bandwidth B_l is usually chosen proportional to the center frequency, such that the filter has a constant Q factor. The octave bandwidth is then also constant and is typically chosen in the range 1/10–1/60 octave, [12],[13],[21],[22].

Finally, the filter specifications $\mathcal{S}_{H_l}(t) = \{\omega_{c,l}, B_l, G_{c,l}\}$ have to be translated to a set of filter coefficients $\mathcal{C}_{H_l}(t) = \{b_l^{(0)}(t), b_l^{(1)}(t), b_l^{(2)}(t), a_l^{(1)}(t), a_l^{(2)}(t)\}$. Most notch filter design methods are based on a bilinear transform of either an analog notch filter transfer function, e.g., [29],[30], or a digital notch filter transfer function centered at $\omega_c = \pi/2$ [28]. A novel design procedure for biquadratic notch filters was recently proposed, that operates directly in the digital domain using a technique known as pole-zero placement [27], which allows for an equally accurate, yet more intuitive design. The complete notch filter design procedure for the two-stage NHS method is shown schematically in Fig. 3.

3. SIGNAL FEATURES FOR HOWLING DETECTION

Six spectral and temporal features of the microphone signal have been proposed to determine whether a candidate howling component with radial frequency $\breve{\omega}_i$ indeed corresponds to a howling component or rather to a source signal tonal component (i.e., a voiced speech or tonal audio component):

1. Peak-to-Threshold Power Ratio (PTPR) [14], [15],[19]: a spectral feature that determines the ratio of the candidate howling component power $|Y(\breve{\omega}_i, t)|^2$ and a fixed absolute power threshold P_0, i.e.,

$$\mathrm{PTPR}(\breve{\omega}_i, t)\ [\mathrm{dB}] = 10 \log_{10} \frac{|Y(\breve{\omega}_i, t)|^2}{P_0}. \quad (6)$$

   The rationale behind using the PTPR for howling detection is that howling should only be suppressed when it appears with a minimum loudness [19]. The absolute power threshold P_0 depends on the particular sound reinforcement scenario at hand, e.g., a value of $10 \log_{10} P_0 = 85$ dB SPL was suggested in [19] for a loudspeaker-microphone distance of 1 m.
2. Peak-to-Average Power Ratio (PAPR) [5],[6], [14]-[16],[18]-[23]: a spectral feature that determines the ratio of the candidate howling component power $|Y(\breve{\omega}_i, t)|^2$ and the average micro-

$$\mathrm{IMSD}(\breve{\omega}_i,t) = \frac{1}{Q_M-1}\sum_{m=1}^{Q_M-1}\left[\frac{1}{Q_M}\sum_{j=0}^{Q_M-1}\frac{1}{Q_M-j}\left(20\log_{10}|Y(\breve{\omega}_i,t-jP)| - 20\log_{10}|Y(\breve{\omega}_i,t-Q_MP)|\right)\right.$$
$$\left. -\frac{1}{m}\sum_{j=0}^{m-1}\frac{1}{m-j}\left(20\log_{10}|Y(\breve{\omega}_i,t-jP)| - 20\log_{10}|Y(\breve{\omega}_i,t-mP)|\right)\right]. \quad (5)$$

phone signal power $\hat{P}_y(t)$, i.e.,

$$\mathrm{PAPR}(\breve{\omega}_i,t)\ [\mathrm{dB}] = 10\log_{10}\frac{|Y(\breve{\omega}_i,t)|^2}{\hat{P}_y(t)} \quad (7)$$

with

$$\hat{P}_y(t) = \frac{1}{M}\sum_{k=0}^{M-1}|Y(\omega_k,t)|^2. \quad (8)$$

This feature exploits the fact that howling may eventually have large power compared to speech and audio components.

3. Peak-to-Harmonic Power Ratio (PHPR) [12]-[15]: a spectral feature that determines the ratio of the candidate howling component power $|Y(\breve{\omega}_i,t)|^2$ and its mth (sub-)harmonic component power $|Y(m\breve{\omega}_i,t)|^2$, i.e.,

$$\mathrm{PHPR}(\breve{\omega}_i,t,m)\ [\mathrm{dB}] = 10\log_{10}\frac{|Y(\breve{\omega}_i,t)|^2}{|Y(m\breve{\omega}_i,t)|^2}. \quad (9)$$

The existence of a harmonic spectral structure is a characteristic property of voiced speech and tonal audio components. Howling does not exhibit this structure, unless the amplifier or loudspeaker is driven into saturation.

4. Peak-to-Neighboring Power Ratio (PNPR) [4], [8]-[10]: a spectral feature that determines the ratio of the candidate howling component power $|Y(\breve{\omega}_i,t)|^2$ and its mth neighboring frequency component power $|Y(\breve{\omega}_i+2\pi m/M,t)|^2$, i.e.,

$$\mathrm{PNPR}(\breve{\omega}_i,t,m)[\mathrm{dB}] = 10\log_{10}\frac{|Y(\breve{\omega}_i,t)|^2}{|Y(\breve{\omega}_i+2\pi m/M,t)|^2}. \quad (10)$$

Since voiced speech and tonal audio components can be represented as damped sinusoids, these components have a non-zero bandwidth and their power is spread over multiple DFT bins around a spectral peak. On the other hand, howling is a purely sinusoidal signal, having its power concentrated in a single DFT bin (if appropriate windowing is applied).

5. Interframe Peak Magnitude Persistence (IPMP) [2],[3],[12],[13],[16],[18],[20]: a temporal feature based on counting in how many frames out of Q_M past signal frames the frequency $\breve{\omega}_i$ is in the set of candidate howling frequencies, i.e.,

$$\mathrm{IPMP}(\breve{\omega}_i,t) = \frac{\sum_{j=0}^{Q_M-1}\left[\breve{\omega}_i \in \mathcal{D}_{\breve{\omega}}(t-jP)\right]}{Q_M}. \quad (11)$$

This feature relies on the observation that howling typically persists for a much longer time than voiced speech or tonal audio components.

6. Interframe Magnitude Slope Deviation (IMSD) [8]-[10]: a temporal feature that determines the deviation (over Q_M successive signal frames) of the slope, which is defined by averaging magnitude difference values of a candidate howling component, where the differentiation is carried out between an old signal frame and more recent signal frames, as shown in Eq. (5) at the top of the page. Small values for the IMSD are characteristic of howling components since these exhibit a nearly linear (dB-scale) magnitude increase in time, hence a nearly constant slope can be expected.

4. EVALUATION OF HOWLING DETECTION CRITERIA

With the aim of objectively evaluating the performance of different howling detection criteria, we will describe the howling detection problem in a more formal way. Suppose that a howling detection experiment is carried out using a microphone signal consisting of L samples, such that $T = L/P$ microphone signal frames are available (with P the frame hop size). In each frame, N candidate howling components are selected from the DFT magnitude spec-

trum by a peak picking algorithm. The howling detection procedure thus operates on a data set of TN spectral components, each of which may be considered as a different realization of a random process that either does or does not correspond to a howling component. When evaluating the detection performance, we assume that we know which of these TN components actually correspond to howling ("positive realizations") and which ones do not correspond to howling ("negative realizations"). By operating on the data set of TN components selected by the peak picking algorithm instead of on the entire set of DFT spectra (which would result in TM spectral components, with M the DFT size), the effect of the peak picking is actually excluded from the howling detection performance evaluation. Also, the relative number of positive and negative realizations in the set of TN components can be balanced somewhat by properly choosing N.

For each of the TN spectral components in the data set, the corresponding howling detection problem can be formulated as a binary hypothesis test [24, Ch. 3], i.e.,

$\mathcal{H}_0$: howling does not occur (Null hypothesis)

$\mathcal{H}_1$: howling does occur (Alternative hypothesis)

The outcome of a howling detection criterion is either that the null hypothesis is rejected (i.e., howling is detected) or the null hypothesis is not rejected (i.e., howling is not detected). The probability of detection (P_D) for a certain howling detection criterion can then be defined as the probability that the null hypothesis is rejected for a positive realization,

$$P_D = P(\mathcal{H}_1;\mathcal{H}_1). \tag{12}$$

This probability can be calculated by counting the number of "true positives" (N_{TP}), i.e., the number of howling components in the data set for which the null hypothesis has been rejected, and dividing by the number op positive realizations in the data set (N_P),

$$P_D = \frac{N_{TP}}{N_P}. \tag{13}$$

On the other hand, the probability of false alarm (P_{FA}) is defined as the probability that a certain howling detection criterion leads to the rejection of the null hypothesis for a negative realization,

$$P_{FA} = P(\mathcal{H}_1;\mathcal{H}_0) \tag{14}$$

and can be calculated by dividing the number of "false positives" (N_{FP}), i.e., the number of non-howling components in the data set for which the null hypothesis has been rejected, by the number of negative realizations in the data set (N_N),

$$P_{FA} = \frac{N_{FP}}{N_N}. \tag{15}$$

A high probability of detection is required for the reliable operation of a sound reinforcement system, such that howling is quickly detected and suppressed by activating appropriate notch filters. On the other hand, a low probability of false alarm is beneficial to sound quality, since a false alarm may result in the suppression of a source signal tonal component. The trade-off between P_D and P_{FA} is governed by the value of the detection threshold. An appropriate threshold value can be selected by plotting P_D vs. P_{FA} for different threshold values, which results in the so-called receiver operating characteristic (ROC) curve [24, Ch. 3]. The ROC curve can also be used to quantify the overall performance of a howling detection criterion, regardless of the threshold value, by calculating the area under the ROC curve (i.e., the larger the area, the better the overall performance).

The ROC curves described below have been generated from an experiment in which a closed-loop sound reinforcement system is simulated. In the simulation, the feedback path $F(q,t)$ is a measured 100 ms room impulse response, the source signal is an audio signal fragment, more specifically a 10 s excerpt from the Partita No. 2 in D minor (Allemande) for solo violin by J. S. Bach, and the electro-acoustic forward path $G(q,t)$ contains a broadband gain cascaded with a saturation function. The gain factor is chosen slightly above the MSG, such that a single howling component slowly builds up in the microphone signal. The corresponding microphone signal spectrogram is shown in Fig. 4 (zooming in on the frequency region $f \in [0,3]$ kHz). With $N = 3$, the data set contains $N_P = 166$ positive realizations and $N_N = 482$ negative realizations.

4.1. Single-feature howling detection criteria

Each of the six signal features described in Section 3 can be used to define a single-feature howling detection criterion:

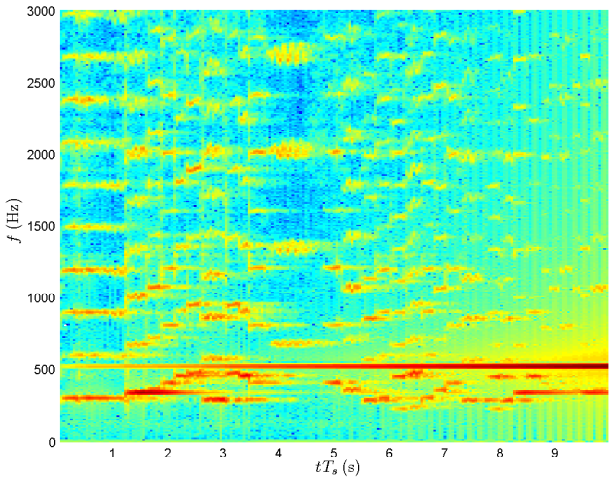


Fig. 4: Microphone signal spectrogram after feeding an audio source signal to a simulated unstable closed-loop system (zooming in on the frequency region $f \in [0, 3]$ kHz).

1. PTPR criterion:

$$\mathrm{PTPR}(\breve{\omega}_i, t) \geq T_{\mathrm{PTPR}}[\mathrm{dB}] \Rightarrow \text{Reject } \mathcal{H}_0 \quad (16)$$

The ROC curve for the PTPR criterion is shown in Fig. 5(a) for $T_{\mathrm{PTPR}} \in (-\infty, +\infty)$ dB and $P_0 = 0$ dB.

2. PAPR criterion:

$$\mathrm{PAPR}(\breve{\omega}_i, t) \geq T_{\mathrm{PAPR}}[\mathrm{dB}] \Rightarrow \text{Reject } \mathcal{H}_0 \quad (17)$$

The PAPR criterion is probably the most widely used howling detection criterion, and different values for the threshold have been proposed, e.g., $T_{\mathrm{PAPR}} = 6$ dB [5],[6], $T_{\mathrm{PAPR}} = 10\log_{10}(M/150)^2$ dB [19], and $T_{\mathrm{PAPR}} = 10$ dB [20]. The ROC curve for the PAPR criterion is shown in Fig. 5(b) for $T_{\mathrm{PAPR}} \in (-\infty, +\infty)$ dB. The area under the ROC curve is clearly larger for the PAPR criterion compared to the PTPR criterion.

3. PHPR criterion:

$$\bigcap_{m \in \mathcal{M}_{\mathrm{PHPR}}} \left[\mathrm{PHPR}(\breve{\omega}_i, t, m) \geq T_{\mathrm{PHPR}}[\mathrm{dB}]\right] \Rightarrow \text{Reject } \mathcal{H}_0 \quad (18)$$

In this criterion, multiple PHPR features are combined for different harmonic indices m. In [12],[13], howling detection is performed with $\mathcal{M}_{\mathrm{PHPR}} = \{0.5, 1.5, 2, 3, 4\}$ and $T_{\mathrm{PHPR}} = 33$ dB, while in [14],[15], a simpler PHPR criterion is used with $\mathcal{M}_{\mathrm{PHPR}} = \{2\}$. The ROC curves for the PHPR criterion are shown in Fig. 5(c) for $T_{\mathrm{PHPR}} \in (-\infty, +\infty)$ dB and for different choices of $\mathcal{M}_{\mathrm{PHPR}}$. It appears that the use of subharmonics (i.e., $m \in \{0.5, 1.5\}$) is not beneficial to the detection performance. The PHPR criterion yields the largest area under the ROC curve among all single-feature howling detection criteria.

4. PNPR criterion:

$$\bigcap_{m \in \mathcal{M}_{\mathrm{PNPR}}} \left[\mathrm{PNPR}(\breve{\omega}_i, t, m) \geq T_{\mathrm{PNPR}}[\mathrm{dB}]\right] \Rightarrow \text{Reject } \mathcal{H}_0 \quad (19)$$

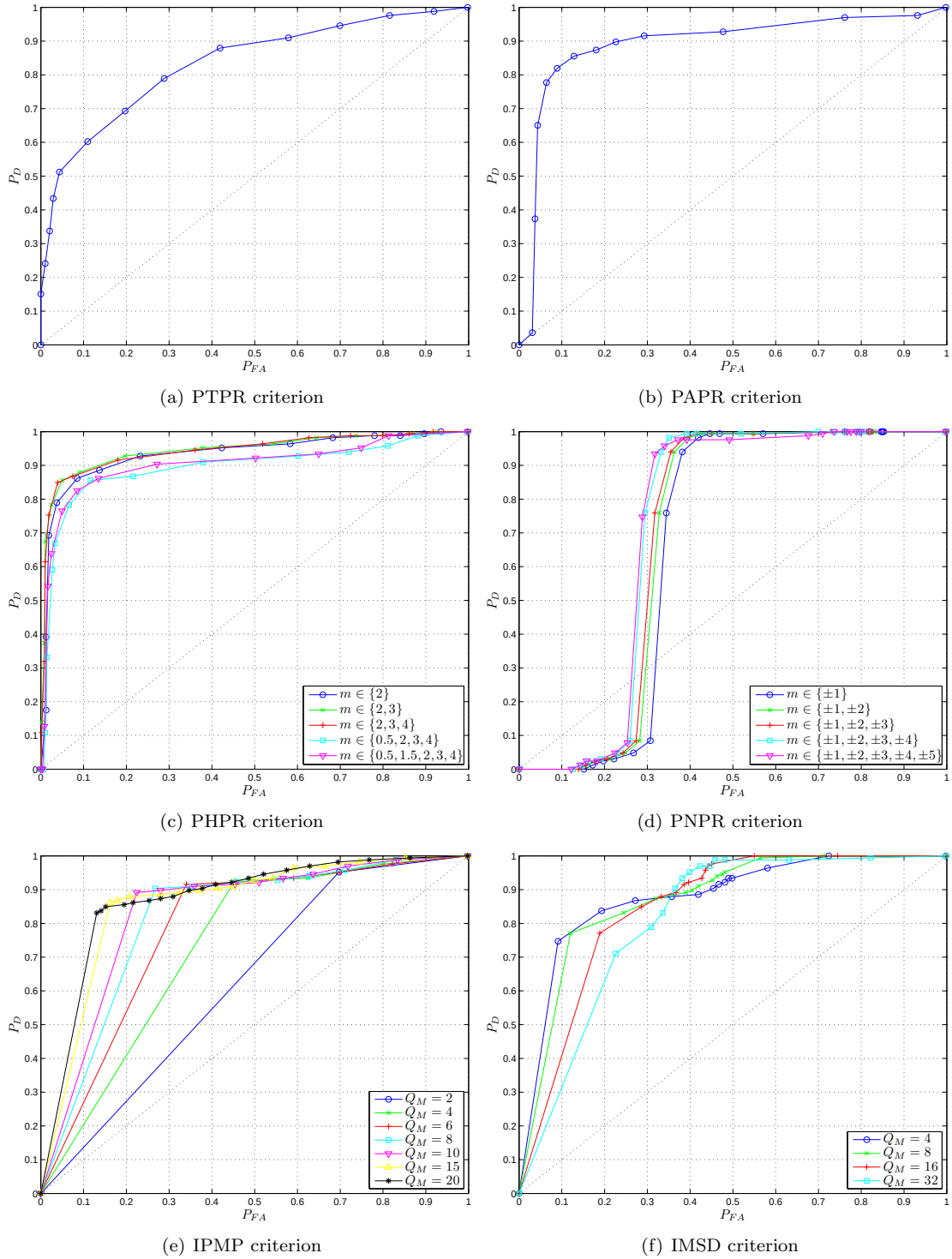
The PNPR criterion incorporates multiple PNPR features, calculated for different neighboring frequency bins around a candidate howling component. In [4], different thresholds $T_{\mathrm{PNPR}}(|m|)$ were used for different neighbors, with $\mathcal{M}_{\mathrm{PNPR}} = \{\pm 1, \pm 2\}$. In [8]-[10], howling is detected based on a so-called "peakness" feature, which reflects the time-averaged probability (over 8 signal frames) that the PNPR, averaged over 6 neighboring frequency bins on either side of $\breve{\omega}_i$ (excluding the closest neighbor on either side), exceeds a 15 dB threshold, i.e.,

$$\begin{aligned}&\mathrm{peakness}(\breve{\omega}_i, t) = \quad (20)\\ &\sum_{j=0}^{7} \frac{1}{16} \left\{ \left[\frac{1}{6} \sum_{m=2}^{7} \mathrm{PNPR}(\breve{\omega}_i, t - jP, m) \geq 15 \text{ dB} \right] \right.\\ &\left. + \left[\frac{1}{6} \sum_{m=-7}^{-2} \mathrm{PNPR}(\breve{\omega}_i, t - jP, m) \geq 15 \text{ dB} \right] \right\}.\end{aligned}$$

The ROC curves for the PNPR criterion are shown in Fig. 5(d) for $T_{\mathrm{PNPR}} \in (-\infty, +\infty)$ dB and for different choices of $\mathcal{M}_{\mathrm{PNPR}}$. In the threshold range where the ROC curves fall below the dotted diagonal line, the PHPR criterion is not appropriate since $P_{FA} > P_D$. This may be due to the spectral leakage of high-power howling components into neighboring DFT bins.

5. IPMP criterion:

$$\mathrm{IPMP}(\breve{\omega}_i, t) \geq T_{\mathrm{IPMP}} \Rightarrow \text{Reject } \mathcal{H}_0 \quad (21)$$



(a) PTPR criterion

(b) PAPR criterion

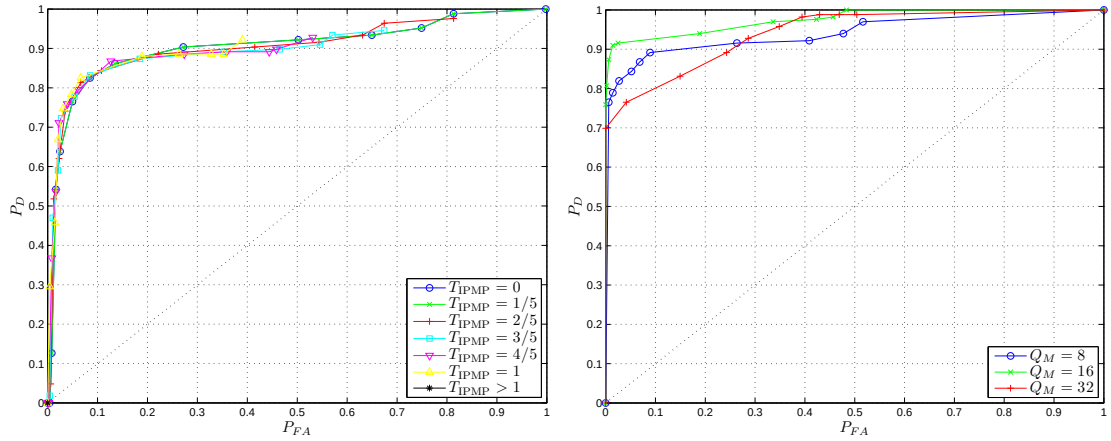
(c) PHPR criterion

(d) PNPR criterion

(e) IPMP criterion

(f) IMSD criterion

Fig. 5: ROC curves for single-feature howling detection criteria.



(a) PHPR & IPMP criterion [12],[13]

(b) FEP criterion [8]-[10]

Fig. 6: ROC curves for existing multiple-feature howling detection criteria.

The IPMP threshold is usually chosen as $T_{\text{IPMP}} = 1$ [2],[3],[16],[18],[20], with, e.g., $Q_M = 3$ [20]. In [12],[13], howling detection is performed with $T_{\text{IPMP}} = 3/5$ and $Q_M = 5$. The ROC curves for the IPMP criterion are shown in Fig. 5(e) for $T_{\text{IPMP}} \in \{0, 1/Q_M, \ldots, (Q_M + 1)/Q_M\}$ and for different choices of Q_M.

6. IMSD criterion:

$$|\text{IMSD}(\breve{\omega}_i, t)| \leq T_{\text{IMSD}}[\text{dB}] \Rightarrow \text{Reject } \mathcal{H}_0 \quad (22)$$

A detection threshold $T_{\text{IMSD}} = 0.05$ dB has been proposed in [10], with $Q_M = 7$. The ROC curves for the IMSD criterion are shown in Fig. 5(f) for $T_{\text{IMSD}} \in [0, +\infty)$ dB and for different choices of Q_M.

4.2. Multiple-feature howling detection criteria

It is obvious that multiple signal features can be combined to obtain howling detection criteria that perform better than the single-feature criteria described above. We will first briefly mention two existing multiple-feature criteria, and then show how improved multiple-feature criteria can be derived by using the information in the ROC curves shown in Fig. 5.

In [12],[13], a multiple-feature howling detection criterion based on the PHPR and IPMP features is proposed, i.e.,

$$\left(\bigcap_{m \in \mathcal{M}_{\text{PHPR}}} \left[\text{PHPR}(\breve{\omega}_i, t, m) \geq T_{\text{PHPR}}[\text{dB}]\right] \right) \wedge \left(\text{IPMP}(\breve{\omega}_i, t) \geq T_{\text{IPMP}}\right) \Rightarrow \text{Reject } \mathcal{H}_0 \quad (23)$$

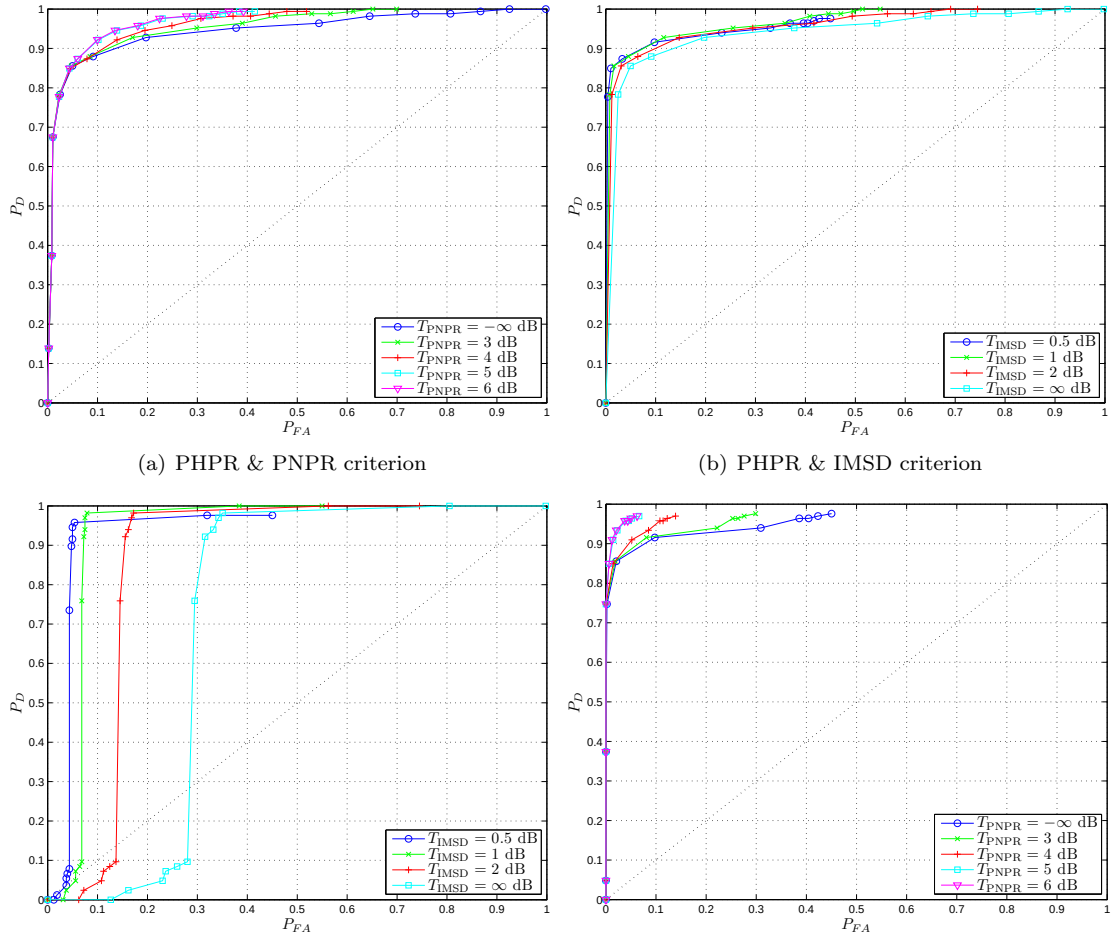
with $\mathcal{M}_{\text{PHPR}} = \{0.5, 1.5, 2, 3, 4\}$ and $Q_M = 5$. The ROC curves for this criterion, corresponding to different values of T_{IPMP}, are shown in Fig. 6(a) for $T_{\text{PHPR}} \in (-\infty, +\infty)$. Comparing this figure with the ROC curve for the PHPR criterion in Fig. 5(c), it can be observed that there is no benefit in adding the IPMP feature to the PHPR criterion. Another multiple-feature howling detection criterion was proposed in [8]-[10], and consists in defining a so-called feedback existence probability (FEP) criterion as follows,

$$\text{FEP}(\breve{\omega}_i, t) \geq T_{\text{FEP}} \Rightarrow \text{Reject } \mathcal{H}_0 \quad (24)$$

with

$$\text{FEP}(\breve{\omega}_i, t) = 0.7 \cdot \text{slopeness}(\breve{\omega}_i, t) + 0.3 \cdot \text{peakness}(\breve{\omega}_i, t). \quad (25)$$

The peakness feature is related to the PNPR feature as in (20), while the slopeness feature is related to the IMSD feature following a nonlinear mapping (which is not explicitly given in [8]-[10], hence we use $\text{slopeness}(\breve{\omega}_i, t) = e^{-|\text{IMSD}(\breve{\omega}_i, t)|}$). The ROC curves obtained with different values for Q_M are shown



(a) PHPR & PNPR criterion

(b) PHPR & IMSD criterion

(c) PNPR & IMSD criterion

(d) PHPR & PNPR & IMSD criterion

Fig. 7: ROC curves for novel multiple-feature howling detection criteria.

in Fig. 6(b), for $T_{\text{FEP}} \in [0, 1]$. The FEP criterion clearly performs better than the single-feature PNPR and IMSD criteria (see Figs. 5(d) and 5(f)).

When deriving novel multiple-feature howling detection criteria, two objectives should be kept in mind. While a high probability of false alarm results in poor sound quality, a low probability of detection is also problematic in terms of sound quality because of howling. Moreover, the closed-loop system stability can be guaranteed only when a high probability of detection is achieved. This suggests that in terms of the overall acoustic feedback control performance, a high probability of detection should be considered more important than a low probability of false alarm. A second issue is that when combining different criteria using a logical conjunction (i.e., the "$\wedge$" operator), the probability of detection of the multiple-feature criterion can never be greater than the probability of detection obtained with the corresponding single-feature criteria. Instead, the effect of a logical conjunction is that the probability of false alarm will decrease compared to the single-feature criteria. As a consequence, we should focus on combining single-feature howling detection criteria that yield a high probability of detection, regardless of their probability of false alarm.

From the above perspective, and by observing the single-feature ROC curves in Fig. 5, we can con-

Table 1: Comparison of probability of false alarm for $P_D = 95$ %

Criterion	$\mathbf{P_{FA}}$	Parameter and threshold values
PTPR	70 %	$P_0 = 0$ dB, $T_{\mathrm{PTPR}} = 34$ dB
PAPR	63 %	$T_{\mathrm{PAPR}} = 35$ dB
PHPR	37 %	$\mathcal{M}_{\mathrm{PHPR}} = \{2, 3\}$, $T_{\mathrm{PHPR}} = 27$ dB
PNPR	33 %	$\mathcal{M}_{\mathrm{PNPR}} = \{\pm1, \pm2, \pm3, \pm4\}$, $T_{\mathrm{PNPR}} = 8$ dB
IPMP	54 %	$Q_M = 20$, $T_{\mathrm{IPMP}} = 6/20$
IMSD	40 %	$Q_M = 32$, $T_{\mathrm{IMSD}} = 0.3$ dB
PHPR & IPMP [12],[13]	65 %	$\mathcal{M}_{\mathrm{PHPR}} = \{0.5, 1.5, 2, 3, 4\}$, $T_{\mathrm{PHPR}} = 10$ dB, $Q_M = 5$, $T_{\mathrm{IPMP}} = 2/5$
FEP [8]-[10]	24 %	$Q_M = 16$, $T_{\mathrm{FEP}} = 0.7$
PHPR & PNPR	14 %	$\mathcal{M}_{\mathrm{PHPR}} = \{2, 3\}$, $T_{\mathrm{PHPR}} = 30$ dB, $\mathcal{M}_{\mathrm{PNPR}} = \{\pm1, \pm2, \pm3, \pm4\}$, $T_{\mathrm{PNPR}} = 6$ dB
PHPR & IMSD	25 %	$\mathcal{M}_{\mathrm{PHPR}} = \{2, 3\}$, $T_{\mathrm{PHPR}} = 27$ dB, $Q_M = 16$, $T_{\mathrm{IMSD}} = 1$ dB
PNPR & IMSD	5 %	$\mathcal{M}_{\mathrm{PNPR}} = \{\pm1, \pm2, \pm3, \pm4\}$, $T_{\mathrm{PNPR}} = 7.5$ dB, $Q_M = 16$, $T_{\mathrm{IMSD}} = 0.5$ dB
PHPR & PNPR & IMSD	3 %	$\mathcal{M}_{\mathrm{PHPR}} = \{2, 3\}$, $T_{\mathrm{PHPR}} = 22$ dB, $\mathcal{M}_{\mathrm{PNPR}} = \{\pm1, \pm2, \pm3, \pm4\}$, $T_{\mathrm{PNPR}} = 6$ dB, $Q_M = 16$, $T_{\mathrm{IMSD}} = 0.5$ dB

clude that particularly the PNPR and IMSD features (and, to a lesser extent, the PHPR feature) are well suited for being combined into a multiple-feature howling detection criterion. In this way, three novel criteria are obtained by pairwise logical conjunction of the PHPR, PNPR, and IMSD criteria given in (18), (19), and (22), respectively, and an additional three-feature criterion results from combining all three PHPR, PNPR, and IMSD features. The corresponding ROC curves are shown in Fig. 7. In each of the four cases, the multiple-feature howling detection criterion clearly outperforms the corresponding single-feature criteria.

Finally, the howling detection performance of all the criteria presented in this paper are compared in Table 1 by fixing the probability of detection to $P_D = 95$ % and calculating the resulting probability of false alarm. The parameter and threshold values used to obtain these results are also given. It can be seen that with the novel multiple-feature criteria, the probability of false alarm can be drastically reduced: $P_{FA} = 5$ % for the PNPR & IMSD criterion and $P_{FA} = 3$ % for the PHPR & PNPR & IMSD criterion.

5. NHS SIMULATION RESULTS

A selection of the existing and novel howling detection criteria presented above has been evaluated in a number of NHS computer simulations. Each simulation consists of four equally long phases, as shown in Fig. 8. In the first phase, the electro-acoustic forward path gain is set to a value K_1 that would result in a 3 dB gain margin if no acoustic feedback control were performed. In the second phase, the gain $20 \log_{10} K(t)$ is then linearly increased up to a value $20 \log_{10} K_2 = 20 \log_{10} K_1 + \Delta K$ beyond the point of instability, with $\Delta K = 5$ dB. In the third and the fourth phase of the simulation, the gain is fixed to K_2, and at the end of the third phase, an acoustic feedback path change due to a 1 m displacement of the microphone is simulated. The source signal is a 60 s audio signal, taken from the same recording as the signal shown in Fig. 4.

In [1], it was observed that a satisfactory NHS performance is obtained only when the howling detection threshold is chosen such as to yield an extremely low probability of false alarm. This observation can be explained by noting that the de-activation of notch filters is an open problem in the NHS literature. As a consequence, every false alarm results in the activation of an unnecessary notch filter that

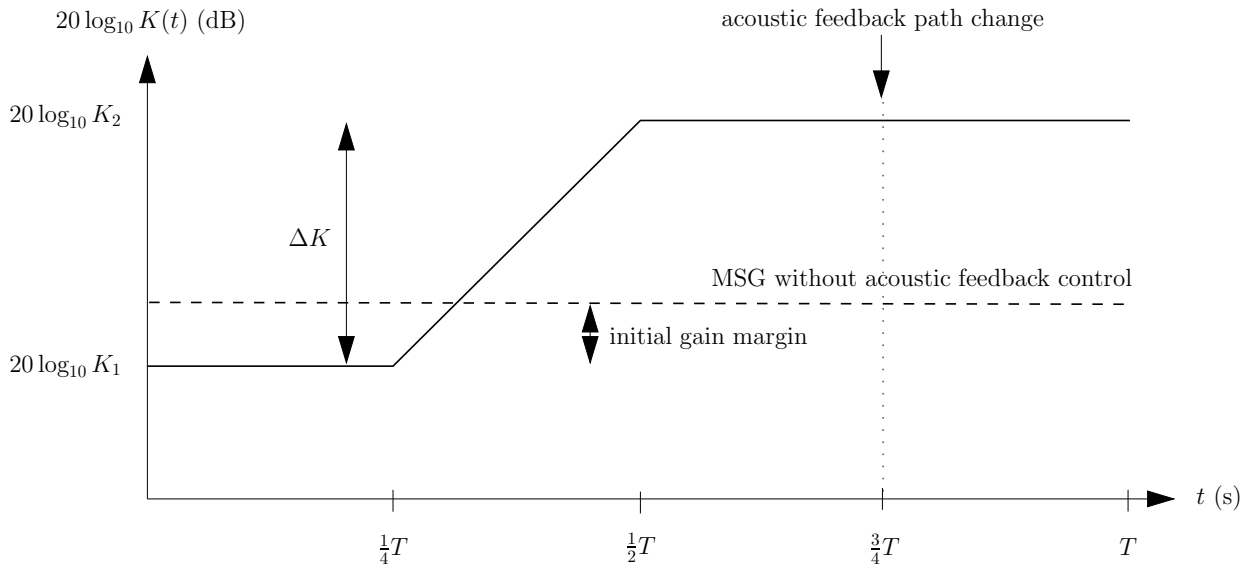


Fig. 8: NHS simulation layout: electro-acoustic forward path gain $20\log_{10} K(t)$ vs. time.

remains active until the end of the simulation. Not only does this affect the sound quality, but it also reduces the number of available notch filters that can be applied when howling does occur. Following this observation, we only include those howling detection criteria in the NHS simulations that are capable of achieving a relatively high probability of detection ($P_D > 65$ %) at a probability of false alarm as low as $P_{FA} = 1$ %. The included criteria are the FEP criterion [8]-[10] (with $T_{\text{FEP}} = 0.9$ and $Q_M = 8$), the PHPR & PNPR criterion (with $T_{\text{PHPR}} = 42$ dB and $T_{\text{PNPR}} = 6$ dB), the PHPR & IMSD criterion (with $T_{\text{PHPR}} = 36$ dB, $T_{\text{IMSD}} = 0.5$ dB and $Q_M = 16$), and the PHPR & PNPR & IMSD criterion (with $T_{\text{PHPR}} = 30$ dB, $T_{\text{PNPR}} = 6$ dB, $T_{\text{IMSD}} = 0.5$ dB and $Q_M = 16$). For the PHPR and PNPR features, we use $\mathcal{M}_{\text{PHPR}} = \{2, 3\}$ and $\mathcal{M}_{\text{PNPR}} = \{\pm1, \pm2, \pm3, \pm4\}$, as before.

The performance of the NHS method is evaluated in terms of three objectives:

1. the achievable amplification is measured by estimating the MSG and the MSG increase (ΔMSG),
2. the sound quality is quantified using a frequency-weighted log-spectral signal distortion (SD) measure [31],
3. the reliability is measured by the howling occurence probability (HOP) and the time to recover from instability (TRI).

We refer to [1] for a formal definition of these performance measures.

In Fig. 9, the instantaneous MSG obtained with an NHS method employing the selected howling detection criteria is plotted as a function of time. The instantaneous electro-acoustic forward path gain $20\log_{10} K(t)$ is also plotted, as well as the MSG values obtained without acoustic feedback control (with "MSG $F_1(q)$" and "MSG $F_2(q)$" denoting the MSG before and after the acoustic feedback path change, respectively). In the time interval where $20\log_{10} K(t) <$ MSG $F_1(q)$ (i.e., for $0 \leq t \leq 23$), the sound reinforcement system is guaranteed to be stable, hence ideally no howling should be detected. However, we observe that the MSG curves for all of the selected howling detection criteria do increase during this time interval, which indicates the occurence of false alarms leading to the activation of unnecessary notch filters. This problem appears to be worse for the PHPR & PNPR & IMSD criterion. When the electro-acoustic forward path gain is increased, the MSG curves increase correpondingly due to the proper activation of notch filters. As long

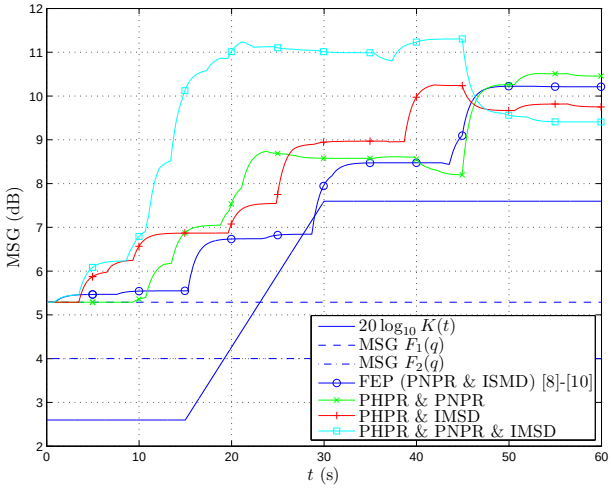


Fig. 9: Instantaneous MSG vs. time for NHS simulations.

as the instantaneous MSG curve stays above the instantaneous gain curve, stability can be guaranteed. This is the case for all of the novel howling detection criteria, but not for the existing FEP criterion, which leaves howling undetected in the time interval $27.7 \leq t \leq 29$. After the feedback path change, the MSG for the FEP and PHPR & PNPR criteria increases due to the proper activation of additional notch filters, while the MSG for the other two criteria decreases because the maximum number of available notch filters (12 in this case) has already been activated earlier.

Table 2 contains the values of the performance measures defined above. The mean and maximum values of the ΔMSG and SD measures have been calculated in the time interval $30 \leq t \leq 60$, which corresponds to the preferential mode of operation of the sound reinforcement system (because it allows for a high electro-acoustic forward path gain). A general observation is that the novel howling detection criteria yield a similar MSG increase and a higher reliability compared to the existing FEP criterion, at the cost of a slight decrease in sound quality. As mentioned before, the PHPR & PNPR & IMSD criterion leads to a relatively high number of false alarms, which explains the poor resulting sound quality. Hence the preferred alternatives to the existing FEP criterion are the PHPR & PNPR and PHPR & IMSD criteria. The howling-compensated signals obtained in the simulations are available for download[2], such that the sound quality can be assessed subjectively by the reader.

6. CONCLUSION

The aim of this paper has been to evaluate existing criteria for howling detection in notch-filter-based howling suppression (NHS) and to propose novel criteria that are particularly suited for audio NHS applications. Six existing signal features have been defined in a formal way and their individual detection performance has been evaluated by inspecting the corresponding receiver operating characteristic (ROC) curves. Multiple-feature howling detection criteria have then been defined by a logical conjunction of single-feature criteria that exhibit a sufficiently high probability of detection. As a result, novel howling detection criteria have been obtained that allow for a drastic decrease of the probability of false alarm for a fixed probability of detection. While the minimum probability of false alarm at $P_D = 95$ % with existing criteria was found to be 33 % for single-feature and 24 % for multiple-feature criteria, the novel criteria can achieve a P_{FA} value as low as 3 %. Finally, a selection of existing and novel howling detection criteria has been evaluated in a number of NHS simulations, in terms of the achievable MSG increase, the sound quality, and the reliability. It appears the the novel criteria in particular deliver a higher reliability compared to the existing criteria, at the cost of a slight decrease in sound quality.

ACKNOWLEDGEMENTS

This research work was carried out at the ESAT laboratory of Katholieke Universiteit Leuven, in the frame of K.U.Leuven Research Council: CoE EF/05/006 Optimization in Engineering (OPTEC) and the Belgian Programme on Interuniversity Attraction Poles initiated by the Belgian Federal Science Policy Office IUAP P6/04 (DYSCO, 'Dynamical systems, control and optimization', 2007-2011), and the Concerted Research Action GOA-AMBioRICS, and was supported by the Institute for the Promotion of Innovation through Science and

[2] ftp://ftp.esat.kuleuven.be/pub/sista/vanwaterschoot/abstracts/08-216.html

Table 2: Performance measures for NHS simulations

	Howling detection criterion			
	FEP [8]-[10]	PHPR & PNPR	PHPR & IMSD	PHPR & PNPR & IMSD
mean(ΔMSG)	4.7	4.8	5.0	5.6
max(ΔMSG)	6.2	6.5	5.8	6.0
mean(SD)	4.4	6.4	4.6	15.7
max(SD)	10.6	13.3	13.5	27.7
HOP (%)	2.2	0	0	0
TRI (s)	0.67	N/A	N/A	N/A

Technology in Flanders (IWT-Vlaanderen). The scientific responsibility is assumed by its authors.

7. REFERENCES

[1] T. van Waterschoot and M. Moonen, "50 years of acoustic feedback control: state of the art and future challenges," *Proc. IEEE*, submitted for publication, Feb. 2009, ESAT-SISTA Technical Report TR 08-13, Katholieke Universiteit Leuven, Belgium. [Online]. Available: ftp.esat.kuleuven.be/pub/sista/vanwaterschoot/abstracts/08-13.html

[2] E. T. Patronis, Jr., "Acoustic feedback detector and automatic gain control," U.S. Patent 4,079,199, Mar., 1978.

[3] ——, "Electronic detection of acoustic feedback and automatic sound system gain control," *J. Audio Eng. Soc.*, vol. 26, no. 5, pp. 323–326, May 1978.

[4] S. Ando, "Howling detection and prevention circuit and a loudspeaker system employing the same," U.S. Patent 6,252,969, June, 2001.

[5] M. Hanajima, M. Yoneda, and T. Okuma, "Howling eliminator," WIPO Patent Application WO/1999/021 396, Apr., 1999.

[6] ——, "Howling eliminating apparatus," U.S. Patent 6,125,187, Sept., 2000.

[7] Y. Terada and A. Murase, "Howling control device and howling control method," U.S. Patent 7,190,800, Mar., 2007.

[8] N. Osmanovic and V. Clarke, "Acoustic feedback cancellation system," U.S. Patent Application 2007/0 019 824 A1, Jan., 2007.

[9] ——, "Acoustic feedback cancellation system," WIPO Patent Application WO/2007/013 981, Feb., 2007.

[10] N. Osmanovic, V. E. Clarke, and E. Velandia, "An in-flight low latency acoustic feedback cancellation algorithm," in *Preprints AES 123rd Convention*, New York, NY, USA, Oct. 2007, AES Preprint 7266.

[11] J. B. Foley, "Adaptive periodic noise cancellation for the control of acoustic howling," in *Proc. IEE Colloq. Adaptive Filters*, London, UK, Mar. 1989, pp. 7/1–7/4.

[12] D. M. Oster, M. P. Lewis, and T. J. Tucker, "Method and apparatus for adaptive audio resonant frequency filtering," WIPO Patent Application WO/1991/020 134, Dec., 1991.

[13] M. P. Lewis, T. J. Tucker, and D. M. Oster, "Method and apparatus for adaptive audio resonant frequency filtering," U.S. Patent 5,245,665, Sept., 1993.

[14] M. H. Er, T. H. Ooi, L. S. Li, and C. J. Liew, "A DSP-based acoustic feedback canceller for public address systems," in *Proc. Int. Conf. Signal Process. (ICSP '93)*, Beijing, China, Oct. 1993, pp. 1251–1254.

[15] ——, "A DSP-based acoustic feedback canceller for public address systems," *Microprocessors and Microsystems*, vol. 18, no. 1, pp. 39–47, Jan./Feb. 1994.

[16] A. Kawamura, M. Matsumoto, M. Serikawa, and H. Numazu, "Sound amplifying apparatus with automatic howl-suppressing function," U.S. Patent 5,442,712, Aug., 1995.

[17] R. Porayath and D. J. Mapes-Riordan, "Acoustic feedback elimination using adaptive notch filter algorithm," U.S. Patent 5,999,631, Dec., 1999.

[18] A. Kawamura, M. Matsumoto, M. Serikawa, and H. Numazu, "Sound amplifying apparatus with automatic howl-suppressing function," European Patent EP0 599 450, Nov., 2001.

[19] P. R. Williams, "Method and system for elimination of acoustic feedback," WIPO Patent Application WO/2002/021 817, Mar., 2002.

[20] A. F. Rocha and A. J. S. Ferreira, "An accurate method of detection and cancellation of multiple acoustic feedbacks," in *Preprints AES 118th Convention*, Barcelona, Spain, May 2005, AES Preprint 6335.

[21] M. Börsch, "Method for constraining electroacoustic feedback," European Patent Application EP1 684 543 A1, July, 2006.

[22] ——, "Method for suppressing electroacoustic feedback," U.S. Patent Application 2006/0 159 282 A1, July, 2006.

[23] D. Somasundaram, "Feedback cancellation in a sound system," European Patent Application EP1 903 833 A1, Mar., 2008.

[24] S. M. Kay, *Fundamentals of statistical signal processing: detection theory.* Upper Saddle River, New Jersey: Prentice-Hall, 1998.

[25] F. J. Harris, "On the use of windows for harmonic analysis with the discrete Fourier transform," *Proc. IEEE*, vol. 66, no. 1, pp. 51–83, Jan. 1978.

[26] J. O. Smith, *Mathematics of the Discrete Fourier Transform (DFT).* `http://ccrma.stanford.edu/~jos/mdft/`, accessed Nov. 2008, online book.

[27] T. van Waterschoot and M. Moonen, "A pole-zero placement technique for designing second-order IIR parametric equalizer filters," *IEEE Trans. Audio Speech Lang. Process.*, vol. 15, no. 8, pp. 2561–2565, Nov. 2007.

[28] J. A. Moorer, "The manifold joys of conformal mapping: Applications of digital filtering in the studio," *J. Audio Eng. Soc.*, vol. 31, no. 11, pp. 826–841, Nov. 1983.

[29] P. A. Regalia and S. K. Mitra, "Tunable digital frequency response equalization filters," *IEEE Trans. Acoust., Speech, Signal Process.*, vol. ASSP-35, no. 1, pp. 118–120, Jan. 1987.

[30] R. Bristow-Johnson, "The equivalence of various methods of computing biquad coefficients for audio parametric equalizers," in *Preprints AES 97th Convention*, San Francisco, CA, USA, Nov. 1994, AES Preprint 3906.

[31] A. Spriet, K. Eneman, M. Moonen, and J. Wouters, "Objective measures for real-time evaluation of adaptive feedback cancellation algorithms in hearing aids," in *Proc. 16th European Signal Process. Conf. (EUSIPCO '08)*, Lausanne, Switzerland, Aug. 2008.